Marginal stability analysis of the phase field crystal model in one spatial dimension

P. K. Galenko*

Institut für Materialphysik im Weltraum, Deutsches Zentrum für Luft- und Raumfahrt (DLR), D-51170 Köln, Germany and Institut für Festkörperphysik, Ruhr-Universität Bochum, D-44780 Bochum, Germany

K. R. Elder

Department of Physics, Oakland University, Rochester, Michigan 48309-4487, USA

(Received 22 October 2010; revised manuscript received 5 January 2011; published 28 February 2011)

The problem of wavenumber k_f and velocity V selection for a solid front invading an unstable homogeneous phase is considered. A marginal stability analysis is used to predict k_f and V for the parabolic and hyperbolic (or modified) phase field crystal models in one dimension. It is shown that the marginally selected wave number of the periodic crystal monotonically increases with increasing undercooling and relaxation times. At high undercooling and relaxation times it is found that the system can select a k_f that is unstable to an Eckhaus instability in the bulk phase. This may imply a transition to highly defected or glassy states in higher dimensions.

DOI: 10.1103/PhysRevB.83.064113 PACS number(s): 05.70.Fh, 05.70.Ln, 64.60.My

I. INTRODUCTION

Determining the selection of patterns that emerge under nonequilibrium conditions is a difficult problem of both technological and fundamental interest. Generally speaking, the selection occurs through the growth of fluctuations from an unstable state or through nucleation from a metastable state and can often occur as a phase front moves through an excitable or unstable media. Important and widely examined examples include the Mullins-Sekerka[1] and Asaro-Tiller-Grinfeld[2] instabilities, side branching in dendrite growth and viscous fingering, convective instabilities, various types of unstable nongradient systems, traveling waves, chemical reactions, and front propagation into unstable states (see overviews in Refs. 3 and 4, and references therein). Of particular interest in this work is the determination of the front velocity and wavelength that emerge as a phase front sweeps through an unstable media.[5]

More specifically, the patterns that emerge behind a front described by the phase field crystal (PFC) model[6] will be examined. The PFC model has been proposed to incorporate the physics naturally embedded on atomic length scales (elasticity, dislocation, etc.) and on diffusive time scales. The PFC model is based on the free-energy functional of the Swift-Hohenberg (SH) form used to describe pattern formation[7] in Rayleigh-Bénard convection. The PFC model describes a field that is related to the local atomic number density, such that it is spatially periodic in the solid and constant in the liquid. It can be related to other continuum field theories such as classical density-functional theory[8,9] and the atomic density function theory.[10] The PFC model may also be considered as a conserved version of the Swift-Hohenberg equation and provides an efficient method for simulating liquid-solid transitions,[11,12] colloidal solidification,[13] dislocation motion and plasticity,[14,15] glass formation,[16] epitaxial growth,[6,17] grain-boundary premelting,[18] surface reconstructions,[19] and grain-boundary energies.[20]

The purpose of this paper is to formulate a method for qualitative and quantitative evaluation of the periodic pattern that emerges as a propagating phase front of a periodic pattern invades an unstable homogeneous supercooled phase. For such purposes the marginal stability analysis of Dee and Langer[5] will be exploited. This analysis is essentially a linear stability analysis around the unstable state in the coordinate frame of the moving front. In this analysis the periodicity and velocity at the propagative front is selected by the mode that is marginally stable and can be used to formulate analytical conditions for dynamic selection rules. Such analysis has been applied to the dynamics described by the Kolmogorov-Fisher and Swift-Hohenberg equations.[21–23] In the present paper this is applied to the PFC model in one dimension for the case in which a stable periodic ("solid") state invades an unstable uniform state.

As originally formulated in a parabolic form, the PFC model allows simulations on diffusive time scales which can be many orders of magnitude larger than molecular dynamics simulations.[6,14] More recently a hyperbolic[24] or modified[25] PFC model was introduced that includes faster degrees of freedom in a form of inertia and as such leads to the description of both fast and slow dynamics. Fast front dynamics proceeds when the driving force for the phase transition is large. This occurs when the free-energy difference between the (meta)stable periodic solid and initially unstable phase is very large, which in general occurs when a system is quenched far below a transition point, or in this case far below the equilibrium temperature of the phase transition.[26] These conditions lead to a fast phase transition when the velocity of the front is comparable to the speed of atomic diffusion or the speed of local structural relaxation. The movement of a phase transition front at such fast velocities can lead to bulk phases that are not in a local structural or chemical equilibrium. As shown,[27] and recently verified in atomistic simulations,[28] the trapping of atoms during rapid movement of the phase interface cannot be described by purely parabolic models. For this reason both parabolic and hyperbolic models of phase field crystals are examined.

The paper is organized as follows. A description of the marginal stability analysis is given in Sec. II. This analysis is then applied to the periodic patterns described by the parabolic and hyperbolic PFC equations in Secs. III and IV, respectively. In Sec. V, a summary of the necessary equations for the qualitative and quantitative predictions of the marginally

selected lattice parameter are given. Interpretations of the selected lattice parameter at the phase front are then presented in Sec. VI for parabolic and hyperbolic PFC equations. Finally, Sec. VII presents a summary of the conclusions.

II. MARGINAL STABILITY ANALYSIS

Consider a front, described by some field ϕ, invading an unstable homogeneous state in the asymptotic time limit. Just ahead of the front ϕ can be expanded around its value in the unstable homogenous state since large deviations from this value only occur behind the front. The marginal stability analysis examines solutions of the linearized equations just ahead of the front in a coordinate frame that is moving with the front, which are of the form $\delta\phi \sim e^{\omega(k)t}$, where $\omega(k)$ is the dispersion relation and k is the wave number. A saddle-point approximation[29] is used to define the complex wave number k^* at the propagating front, i.e.,

$$\left.\frac{\partial\omega}{\partial k}\right|_{k^*} = 0. \tag{1}$$

Together with the dispersion relation $\omega(k)$, Eq. (1) defines the most unstable mode at the front. Assuming the front is stationary in the moving coordinate frame, it must neither grow nor decay exponentially at $k = k^*$, i.e,

$$\mathrm{Re}[\omega(k)|_{k^*}] = 0. \tag{2}$$

The front is oscillating at angular frequency and moving with the linear velocity V. Consequently, the final wave number k_f at the front must be selected as

$$k_f = \frac{\mathrm{Im}[\omega(k^*)]}{V}. \tag{3}$$

Equations (1)–(3) were proposed by Dee and Langer[5] and have been applied to the analysis of state selection when fronts propagate into unstable states.[22] A wide class of pattern propagation equations was investigated using the marginal stability conditions identical to Eqs. (1)–(3) in nonlinear dissipative systems[21] as well as in the asymptotic time regime of phase front dynamics.[23]

Marginal stability analysis essentially reduces to assuming that the equation of motion can be linearized in a moving coordinate frame just ahead of the front, where perturbations in the appropriate field (i.e., the atomic number density) are small. As the front moves by these perturbations increase and nonlinear corrections to the marginal stability predictions may be important. Nevertheless, such analysis provides insight into the selection of states and will be examined for the parabolic and hyperbolic PFC-type linearized systems.

III. PARABOLIC SYSTEM

A. Governing equations and dispersion relation

The parabolic PFC model can be written as[6]

$$\frac{\partial\phi}{\partial t} = \nabla^2\{[-\epsilon + (1+\nabla^2)^2]\phi + \phi^3\} \tag{4}$$

in dimensionless units, where the spatial coordinates are measured in units proportional to the lattice constant and the parameter ϵ is proportional to the undercooling, i.e., $\epsilon \sim T_e - T$, where T_e is the equilibrium temperature for phase transition. This equation can also be written in the form of a continuity equation for a conserved field, i.e.,

$$\frac{\partial\phi}{\partial t} + \vec{\nabla}\cdot\vec{J} = 0, \tag{5}$$

where $\vec{J}$ is the flux given by the steady-state equation $\vec{J} = -\nabla(\delta\mathcal{F}/\delta\phi)$, and $\mathcal{F}$ is a dimensionless free energy given by

$$\mathcal{F}(\phi,\vec{\nabla}\phi) = \int d\vec{r}\left\{\phi[-\epsilon + (1+\nabla^2)^2]\frac{\phi}{2} + \frac{\phi^4}{4}\right\}. \tag{6}$$

In one dimension, Eq. (6) is minimized by a periodic pattern with wave vector $k_b \approx 1 - \epsilon^2/1024$ as predicted in Ref. 30 in the small-ϵ limit. Equation (4) is identical to the Swift-Hohenberg equation[7] except for the outer Laplacian that ensures that the field ϕ is a conserved variable.

To obtain the selected lattice parameter of the periodic pattern at the front, we first expand the order parameter ϕ around the unstable homogeneous state $\phi_0 = 0$, i.e.,

$$\delta\phi = \phi - \phi_0 \quad \text{with} \quad |\delta\phi|/A \ll 1 \tag{7}$$

at the front of periodic pattern invading the unstable phase with the velocity V and the undercooling $\epsilon > 0$, where A is the amplitude of the fluctuations in the bulk periodic phase. This situation is schematically shown in Fig. 1 in which λ represents the characteristic wavelength (or lattice parameter of the crystalline solid) of the periodic pattern. In general the marginally selected wave number k_f at the front will be different from the wave number k_b formed in the bulk crystalline solid, as the selection criteria are different. It is also possible that the selected wave number k_f at the front becomes unstable (or highly metastable) in the bulk phase and will relax to the equilibrium value through an Eckhaus instability.

Linearizing Eq. (4) in coordinate frame moving at velocity V gives

$$\frac{\partial\delta\phi}{\partial t} - V\frac{\partial\delta\phi}{\partial x} = \alpha(\nabla^2)\delta\phi, \tag{8}$$

where

$$\alpha(\nabla^2) = \nabla^2[-\epsilon + (1+\nabla^2)^2]. \tag{9}$$

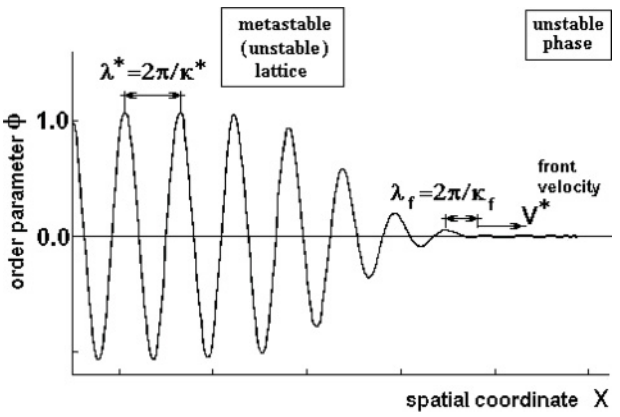

FIG. 1. Crystalline phase invading an unstable phase. Propagating oscillatory pattern with the front velocity V reproduces the periodic structure of solid-crystal lattice (left) by the front invading the unstable phase (right).

Assuming a one-dimensional solution of Eq. (8) in the form

$$\delta\phi = A\exp(\omega t + ikx) + \text{c.c.} \tag{10}$$

gives

$$\omega(k) = ikV + \alpha(k), \tag{11}$$

where c.c. is the complex conjugate. Using the dispersion relation (11), Eq. (9) transforms into

$$\alpha(k) = k^2[\epsilon - (1-k^2)^2]. \tag{12}$$

B. Marginal stability of the phase front

The most unstable mode, with critical wave number k^*, is defined by the saddle-point condition (1), which applied to Eq. (11) gives

$$iV + \left.\frac{d\alpha(k)}{dk}\right|_{k^*} = 0. \tag{13}$$

If the front is to be stationary in the reference coordinate frame moving with the constant velocity V, then the marginal stability condition (2) applied to Eq. (11) gives

$$\text{Re}[ik^*V + \alpha(k^*)] = 0. \tag{14}$$

Equation (14) defines the condition at which the perturbation $\delta\phi$ neither grows or decays at wave number k^* near the front. Since Eq. (13) is complex it represents two equations and combined with Eq. (14) allows for solution of the velocity V and the wave number k^* which is complex:

$$k^* = k^*_{\text{Re}} + ik^*_{\text{Im}}, \tag{15}$$

where k^*_{Re} and k^*_{Im} are the real and imaginary parts, respectively.

Selection of the wave number k_f at the front oscillating at angular frequency $\text{Im}[\omega(k^*)]$ is defined by Eq. (3). Therefore, using the dispersion relation (11), one obtains

$$k_f = V^{-1}\text{Im}[ik^*V + \alpha(k^*)]. \tag{16}$$

Solution of Eqs. (13)–(16) is not possible analytically so a numerical solution is required.[31]

IV. HYPERBOLIC SYSTEM

A. Governing equation

To take large deviations from thermodynamic equilibrium into account a model for fast phase transitions[32] has been proposed by modifying the phase field crystal model.[24] By incorporating fast degrees of freedom it is possible to make predictions at large undercoolings and for the earliest stages of evolution. Choosing the flux $\vec{J}$ as the fast variable, the nonequilibrium part of the free energy becomes

$$\mathcal{F}_{ne}(\vec{J}) = \frac{\tau}{2}\int \vec{J}\cdot\vec{J}\,d\vec{r}, \tag{17}$$

where τ is the dimensionless time for relaxation of the flux $\vec{J}$ to the steady state. The relaxation time τ is assumed to be positive, because pure nonequilibrium contribution should lead to an increase of the free energy in comparison with Eq. (6). In general, the nonequilibrium contribution (17) is related to the kinetic energy as has been shown in the example of phase separation by the mechanism of spinodal decomposition.[33]

The condition that the total free energy must decrease in time, $d\mathcal{F}/dt + d\mathcal{F}_{ne}/dt < 0$, for Eqs. (6) and (17), leads to the following evolution equation:

$$\tau\frac{\partial\vec{J}}{\partial t} + \vec{J} = -\vec{\nabla}\left(\frac{\delta\mathcal{F}}{\delta\phi}\right). \tag{18}$$

Substituting Eq. (18) into balance law (5) gives the hyperbolic (modified) PFC equation:

$$\tau\frac{\partial^2\phi}{\partial t^2} + \frac{\partial\phi}{\partial t} = \nabla^2\{[-\epsilon + (1+\nabla^2)^2]\phi + \phi^3\}. \tag{19}$$

Equation (19) shows that, in addition to the dissipation described by the parabolic PFC equation (4), inertia $\propto \partial^2\phi/\partial t^2$ is also taken into account due to kinetic contribution (17). Alternatively, Eq. (19) was proposed by Stefanovic *et al.*[25] to incorporate both fast elastic relaxation and slower mass diffusion.

Linearizing Eq. (19) in $\delta\phi$ gives

$$\tau\frac{\partial^2\delta\phi}{\partial t^2} + \frac{\partial\delta\phi}{\partial t} = \alpha(\nabla^2)\delta\phi, \tag{20}$$

where the operator $\alpha(\nabla^2)$ is defined by Eq. (9). Before conducting a marginal stability analysis of this equation near the front, some basic features of this equation will be discussed in the next section.

B. Dispersion relation and particular solution

Substituting Eq. (10) into Eq. (20) gives

$$\tau\omega^2 + \omega - \alpha(k) = 0, \tag{21}$$

or

$$\omega_\pm = \frac{1}{2\tau}[\pm\sqrt{1+4\tau\alpha(k)} - 1], \tag{22}$$

where $\alpha(k)$ is the same as given by Eq. (12). As expected, when $\tau \to 0$ this equation reduces to the parabolic solution $\omega_\pm \equiv \omega = \alpha(k)$, at $V = 0$, consistent with Eq. (11).

The solution of interest is ω_+ since it describes the fastest growing modes and is maximized when $d\omega_+/dk = 0$, or in this instance when $d\alpha/dk = 0$. Solving $d\alpha/dk = 0$ gives

$$k_m = 0, \quad \text{and} \quad k_m = \frac{\sqrt{3}}{3}\sqrt{2+\sqrt{4+3(\epsilon-1)}}, \tag{23}$$

with the condition $\alpha \neq -1/(4\tau)$. Note that the values of $\omega_+(k_m)$ and k_m do not depend on the relaxation time τ that characterizes local nonequilibrium phenomena. This is quite logical because the final state of the ϕ-field evolution should be in local thermodynamic equilibrium.

The linear solution for the ω_+ can be written

$$\delta\phi(x,t) = Ae^{\sqrt{1+4\tau\alpha(k)}\,t/2\tau}e^{-t/2\tau}e^{ikx} + \text{c.c.} \tag{24}$$

When $1 + 4\tau\alpha(k) < 0$ this solution describes underdamped time oscillations that decay exponentially on time scales of the order 2τ. This damped oscillatory mode is a feature of fast phase transitions in the hyperbolic Swift-Hohenberg system[24] and a spinodally decomposed system,[34] and does not occur in parabolic equations. Using Eq. (12), the range of k at which

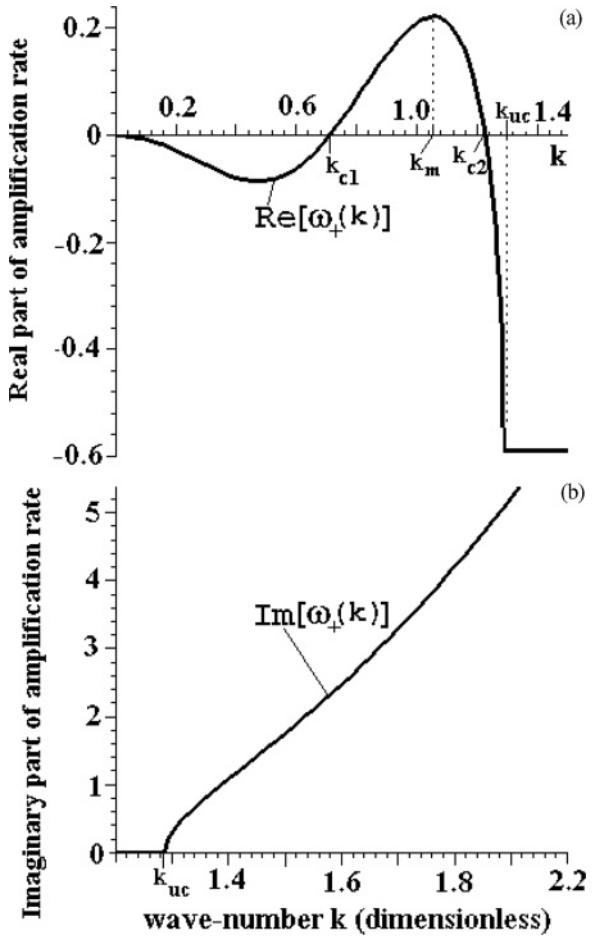

FIG. 2. Amplification rate $\omega_+(k)$ for the hyperbolic PFC equation computed by Eq. (22) with $\epsilon = 0.25$ and $\tau = 0.85$. (a) Real part of amplification rate, $\mathrm{Re}[\omega_+]$. Here, values for k_c are given by solution for $\alpha_+(k) = 0$, one of maxima at $k_m \approx 1.05$ is given by Eq. (23), and region $k > k_{uc}$ is given by inequality (25). (b) Imaginary part of amplification rate, $\mathrm{Im}[\omega_+]$, existing at $k > k_{uc}$.

solution (24) becomes oscillatory (or ω_+ becomes complex) is given by the following inequality:

$$k^6 - 2k^4 + (1-\epsilon)k^2 - (4\tau)^{-1} > 0. \tag{25}$$

Obviously, the range of imaginary values of ω_+ and $\delta\phi(x,t)$ exists at $k > k_{uc}$, where k_{uc} is the ultraviolet cutoff. The latter gives a boundary for modes having oscillations, i.e., a boundary between real and complex values for the amplification rate.

Figure 2 shows the behavior for $\omega_+(k)$ for sample values of the undercooling ϵ and relaxation time τ. The real part $\mathrm{Re}[\omega_+]$ shown in Fig. 2(a) is positive in the range $k_{c1} < k < k_{c2}$ that leads to instability and growth of fluctuations in the ϕ field. The negative real part $\mathrm{Re}[\omega_+] < 0$ in the ranges $0 < k < k_{c1}$ and $k > k_{c2}$ presents a stable mode for ϕ. $\mathrm{Re}[\omega_+]$ becomes a negative constant behind the ultraviolet cutoff, i.e., at $k > k_{uc}$. The latter range characterizes the increase in the imaginary part $\mathrm{Im}[\omega_+]$ as the wave number increases, Fig. 2(b).

Further analysis of ω_+ can be made with respect to parameters ϵ and τ. First, at a fixed and finite value of τ, this calculation shows that an increase in undercooling ϵ leads to a wider range $k_{c1} < k < k_{c2}$ for instability of ϕ. With $\epsilon > 1$, one has $k_{c1} = 0$ and positive function $\omega_+(k)$ within the range $0 < k < k_{c2}$. Therefore the ϕ field becomes unstable in a whole range of $0 < k < k_{c2}$ at $\epsilon > 1$. On the other hand, with near zero undercooling, i.e., at the thermodynamic equilibrium state with $\epsilon = 0$, the real part of amplification rate is negative, $\mathrm{Re}[\omega_+] < 0$ excluding roots $\omega_+ = 0$ at $k = 0$ and $k = 1$. In this case, the solution for ϕ becomes stable for $\epsilon = 0$ at any k with $k \neq 0$ and $k \neq 1$. Second, at a fixed and finite value of ϵ, the decrease of relaxation time τ shifts the imaginary part $\mathrm{Im}[\omega_+]$ to the region of larger wave numbers. In the local equilibrium limit, $\tau \to 0$, the imaginary part $\mathrm{Im}[\omega_+]$ completely disappears. In this case, (i) the oscillatory behavior for $\delta\phi$ does not exist according to solution (24), (ii) the order parameter ϕ monotonically evolves in time by the parabolic PFC equation (4) characterizing the local equilibrium dynamics.

C. Propagative speeds

The parabolic PFC equation (4) describes relaxation of the "slow" thermodynamic variable ϕ and predicts low-frequency regimes with long-wave interaction in the periodic pattern. The hyperbolic PFC equation (19) describes relaxation of the slow thermodynamic variable ϕ as well as of the fast variable $\vec{J}$ (in a sense of the model of fast transformations[32] consistent with a general thermodynamics of transport processes[35]). Equation (19) extends the analysis to describe both high-frequency mode and low-frequency mode, i.e., it predicts short-wave and long-wave interaction, respectively. Propagation of the interaction in the evolving periodic pattern can be characterized by the phase speed and group speed. Therefore we consider these speeds to characterize the high- and low-frequency modes assumed by the hyperbolic PFC equation.

The phase speed characterizes propagation of a single monochromatic harmonic and is obtained as $V_p(k) = \omega_+(k)/k$. Using Eqs. (12) and (22), it is given by

$$V_p(k) = \frac{\sqrt{1+4\tau\alpha(k)} - 1}{2\tau k}. \tag{26}$$

Additionally, propagating disturbances of the order parameter ϕ can be characterized by an undistorted wave packet with the group speed $d\omega_+(k)/dk = \pm W(k)$, where the upper and lower signs correspond to the propagation of wave packets in the positive and negative x directions, respectively. Using Eq. (22), the group speed which is moving only in the positive direction of origin, is given by

$$W(k) = \frac{d\alpha/dk}{\sqrt{1+4\tau\alpha(k)}} = \frac{2k\{\epsilon + (1-k^2)(3k^2-1)\}}{\sqrt{1+4\tau\alpha(k)}}. \tag{27}$$

Both speeds (26) and (27) become complex with the inequality $\alpha(k) < -1/(4\tau)$, which holds in the region $k > k_{uc}$, i.e., behind the ultraviolet cutoff given by the wave number $k = k_{uc}$ (25). Also, the group speed (27) diverges at $\alpha(k) = -1/(4\tau)$ and $k = k_{uc}$. These features are shown in Fig. 3, where the real and imaginary parts of the phase and group speeds are presented as a function of the wave number k for fixed values of undercooling $\epsilon = 0.5$ and relaxation time $\tau = 2.0$. The appearance of imaginary components of $V_p(k)$

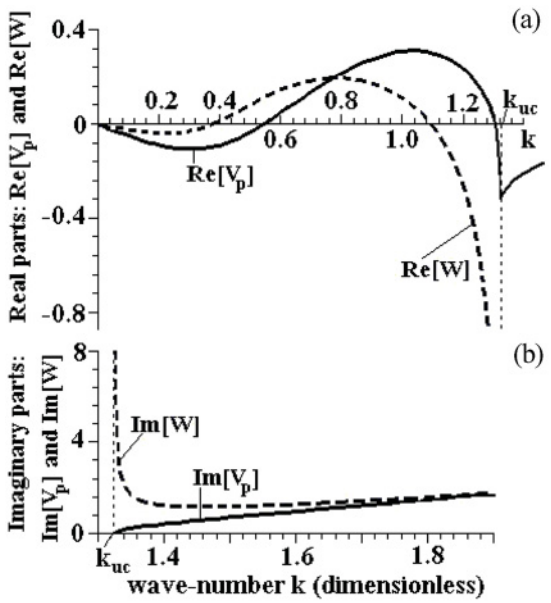

FIG. 3. Phase and group speeds for hyperbolic PFC equation computed by Eqs. (26) and (27), respectively, with $\epsilon = 0.5$ and $\tau = 2.0$. (a) Real part $\mathrm{Re}[V_p(k)]$ of phase speed (solid line) and real part $\mathrm{Re}[W(k)]$ of group speed (dashed line). (b) Imaginary part $\mathrm{Im}[V_p(k)]$ phase speed (solid line) and imaginary part $\mathrm{Im}[W(k)]$ of group speed (dashed line), existing at $k > k_{uc}$.

and $W(k)$ means that the propagation of interaction by the dispersion law (22) proceeds with changing amplitude for both single harmonics and wave packet at high k values consistent with the high-frequency mode. This mode is also consistent with the oscillatory solution (24) at the high frequency, $\alpha(k) < -1/(4\tau)$ and $k > k_{uc}$. Such a regime is absent for the parabolic PFC equation in which these speeds are always real:

$$V_p(k)|_{\tau\to 0} = \frac{\alpha(k)}{k}, \quad W(k)|_{\tau\to 0} = \frac{d\alpha}{dk}, \tag{28}$$

as predicted by Eqs. (26) and (27) for the local equilibrium limit $\tau \to 0$. Thus one can characterize the behavior of ϕ in the hyperbolic PFC equation (19) as an oscillatory relaxation in the high-frequency (short-wave) regime and monotonic relaxation to equilibrium in the low-frequency (long-wave) regime.

V. SELECTION OF THE LATTICE PARAMETER

The lattice parameter λ of the periodic pattern described by the PFC model can be obtained by the specific wave number k as $\lambda = 2\pi/k$. Now the marginal stability analysis from Sec. II will be used to predict lattice parameter selection in the hyperbolic system. Consider Eq. (20) in the moving reference frame with the origin at the front invading unstable phase. Then, in Eq. (20), both transformations for time derivatives being considered $\partial(\delta\phi)/\partial t = \partial(\delta\phi)/\partial t - V\partial(\delta\phi)/\partial x$ and $\partial^2(\delta\phi)/\partial t^2 = \partial^2(\delta\phi)/\partial t^2 - 2V\partial^2(\delta\phi)/\partial t\partial x + V^2\partial^2(\delta\phi)/\partial x^2$. In this case, the one-dimensional linearized hyperbolic PFC equation is given by

$$\tau\frac{\partial^2\delta\phi}{\partial t^2} - 2\tau V\frac{\partial^2\delta\phi}{\partial t\partial x} + \frac{\partial\delta\phi}{\partial t} = \frac{\partial^2}{\partial x^2}\left[-(\tau V^2+\epsilon) + \left(1+\frac{\partial^2}{\partial x^2}\right)^2\right]\delta\phi + V\frac{\partial\delta\phi}{\partial x}. \tag{29}$$

Assuming a solution of the form given in Eq. (10), the dispersion relation obtained from Eq. (29) is then

$$\tau\omega^2 + (1 - 2i\tau Vk)\omega = \tau V^2k^2 + iVk + \alpha(k) \tag{30}$$

with $\alpha(k)$ given by Eq. (12). Equation (30) shows that, in the high-frequency limit (high ω and high V at large ϵ), the term $2i\tau Vk$ may have significance in comparison with unity.[36] Solution of Eq. (30) gives the following amplification rate:

$$\omega_+ = \frac{1}{2\tau}[\sqrt{1+4\tau\alpha(k)} - 1] + iVk. \tag{31}$$

Two limits for Eq. (31) can be outlined: (i) the equation transforms into amplification rate ω_+ from Eq. (22) in the fixed laboratory system of coordinates, $V = 0$, and (ii) the equation transforms into dispersion relation (11) in the local equilibrium limit $\tau \to 0$.

The marginal stability criterion (2) together with the amplification rate (31) gives the front velocity as

$$V = \frac{1}{k^*_{im}}\mathrm{Re}\left\{\frac{1}{2\tau}[\sqrt{1+4\tau\alpha(k^*)} - 1]\right\}, \tag{32}$$

where k^* is the selected wave number assumed to be complex valued, Eq. (15). The critical wave number given by the saddle point (1) is obtained by Eq. (31) as

$$\left.\frac{d\omega_+}{dk}\right|_{k^*} = 0 = iV + \frac{2k^*[\epsilon - 1 + 4(k^*)^2 - 3(k^*)^4]}{\sqrt{1+4\tau\alpha(k^*)}}. \tag{33}$$

Finally, the angular frequency selects the wave number at the front by Eq. (3). As in the case of parabolic PFC dynamics, the system of equations (32), (33), and (3) should be solved numerically.

VI. DISCUSSION

In this section numerical results for the wave number and front velocity for the parabolic and hyperbolic equations are presented and discussed. Figure 4 show solutions for the front velocity V and the selected wave number k_f as functions of the undercooling ϵ given by the parabolic PFC model (with $\tau = 0$) and the hyperbolic PFC model (with the finite value of τ). As shown in Fig. 4(a), the front velocity V predicted by the parabolic PFC model is always higher than that predicted by the hyperbolic PFC model for positive ϵ.

The parabolic PFC model predicts lower values for the selected wave number $k_f^{(p)}$ in comparison with the wave number $k_f^{(h)}$ predicted by the hyperbolic PFC model as is shown in Fig. 4(b) for finite ϵ. In this case, the lattice parameter $\lambda_f^{(p)}$, marginally selected by the parabolic PFC model, should

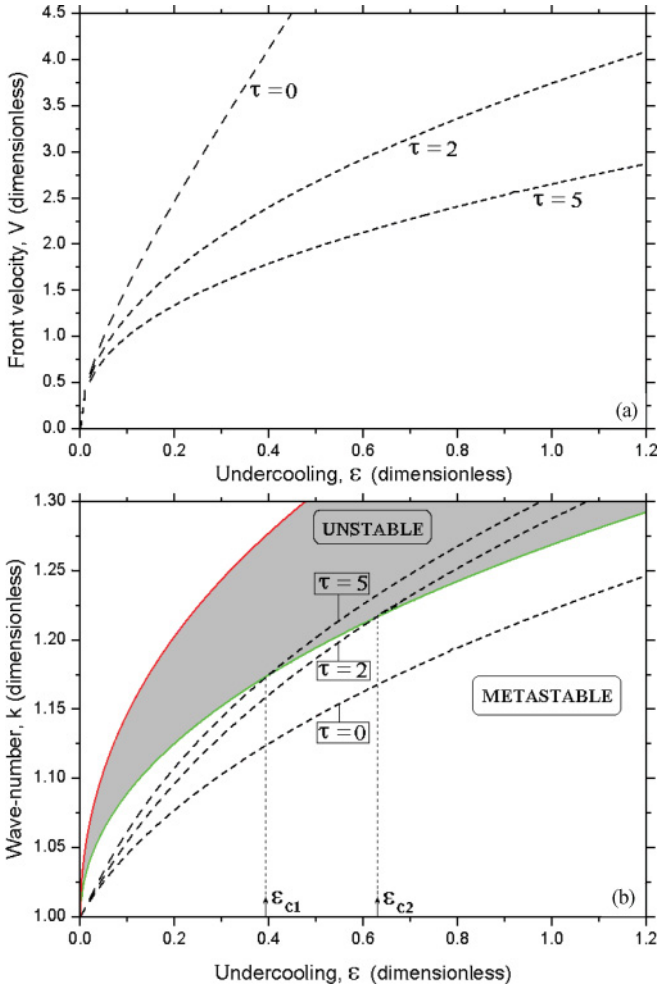

FIG. 4. (Color online) Quantitative predictions of the PFC model: (a) the front velocity V and (b) the wave number k_f at the front of periodic pattern (qualitative scheme for these parameters is shown in Fig. 1). Marginal stability predictions are made for parabolic system with $\tau = 0$, and the hyperbolic model with $\tau = 2$ and $\tau = 5$. The dashed region in (b) corresponds to a region of Eckhaus instability.

be greater than the lattice parameter $\lambda_f^{(h)}$ predicted by the hyperbolic PFC model:

$$\lambda_f^{(p)} = 2\pi/k_f^{(p)} > \lambda_f^{(h)} = 2\pi/k_f^{(h)}. \tag{34}$$

The tendency given by Eq. (34) might be tested in molecular-dynamic simulations or in experimental findings for the freezed metastable phases undergoing a fast phase transition. Thus atomistic modeling or experimental data on the front velocity and lattice parameter may give independent tests of the predictions of the parabolic and hyperbolic models, especially in a high-velocity regime of phase transition.

At the smallest values of undercooling $0 \leqslant \epsilon < 0.05$ both PFC models predict the same values for V and k_f as is shown in Fig. 4. Therefore the inertial as well as local nonequilibrium phenomena are negligible in the front dynamics of the phase field crystals at small values of undercooling.

In Fig. 4(b), regions of stable, metastable, and unstable periodic patterns are also plotted. These are obtained using a linear analysis of stability around a periodic state as developed in Refs. 24 and 37. Indeed, it is straightforward to show that the stability analysis of the present hyperbolic PFC model, described by Eq. (19), gives the same boundaries for stable-metastable-unstable regions in the "ϵ-k" phase diagram as it is treated for periodic patterns in the parabolic PFC equation[37] and the hyperbolic Swift-Hohenberg equation.[24] As a result of such analysis, the equilibrium[38] value of $k \approx 1$, is obviously always linearly stable. As k deviates from this value (getting larger or smaller) eventually an Eckhaus instability occurs (for details, see Ref. 39). The shaded region in Fig. 4(b) corresponds to a region where this instability occurs, for which the lower bound is

$$\epsilon(k) = \frac{1 - 9k^2 + 15k^4 - 7k^6}{1 - 3k^2}. \tag{35}$$

The upper bound of the shaded region shown in Fig. 4(b) is given by the curve[24,37]

$$\epsilon(k) = (1 - k^2)^2. \tag{36}$$

This curve (36) gives the cut (demarcation line) between the region of Eckhaus instability and the region of absence of real periodic solutions in a one-mode approximation.

As is clearly seen in Fig. 4(b), for parabolic dynamics (with $\tau = 0$) the marginally selected wave number k_f completely lies in a region of metastability. In contrast, for large enough undercooling the wave number selected for hyperbolic dynamics can be in an unstable region, i.e., above the Eckhaus bound. Defining ϵ_c as the critical undercooling below which k_f is metastable and beyond which k_f falls into the unstable region, we find that ϵ_c decreases as τ increases. This implies that for large enough τ the critical undercooling becomes small.

While the analysis provided in the manuscript is a linear analysis around a one-dimensional moving front, it is interesting to speculate about the consequences of wave-number selection for the bulk when k_f is in the unstable region. To continue the discussion it is useful to note that the Eckhaus instability analysis considers the stability of an infinitely long periodic pattern to a perturbation of wavelength Q, i.e., $\delta\phi \sim \sum_n b_n e^{i(nk+Q)x}$, where k is the wave number of the infinitely long periodic pattern. In this analysis it is found that $b_n \sim e^{\omega_{Eck}(Q)t}$, where ω_{Eck} is positive for some range of Q's in the unstable region in Fig. 4(b) and negative for all values of values of Q in the metastable region. In the unstable region the maximum positive value of ω_{Eck} occurs at some value of $Q = Q_{\max}$ that is zero at the boundary between metastable and unstable regions and increases as the system goes deeper into the unstable zone (i.e., as k_f increases). In addition, $\omega_{Eck}(Q_{\max})$ also increases further into unstable zone. With these considerations several possible scenarios or limiting cases can be outlined.

If the selected wave number k_f is just above the metastable zone, then $Q_{\max}$ is small and thus it is possible that the bulk will form at k_f since the instability to change wavelengths can only occur when many wavelengths appear (i.e., so that fluctuations on wavelengths of order $\sim 2\pi/Q_{\max}$ are possible). In this limit $\omega_{Eck}(Q_{\max})$ is relatively small so it may take some time before a phase slip occurs in the bulk region and the system returns to a k value closer to the equilibrium one.

In contrast, when k_f is well into the unstable region, $Q_{\max}$ is larger and the magnitude of $\omega_{Eck}(Q_{\max})$ increases. This implies a much larger likelihood of an Eckhaus instability occurring near the front. If such an instability occurs near to the front then the bulk may form at a wave number closer to the equilibrium value. It should, however, be emphasized that the marginal stability analysis just ahead of the front and the Eckhaus analysis in the bulk are both linear and thus not applicable in the transition zone between the bulk and just ahead of the front. It is possible that nonlinear instabilities can occur and correct the conclusion drawn in this paragraph.

Finally, we stress that the above analysis has been given for the linearized systems described by the parabolic (8) and hyperbolic (29) equations in the limit in which the average value of ϕ is zero. In this instance the transition is second order and the periodic state invades a state that is linearly unstable. This situation occurs in many other systems with long-range interactions, such as in block copolymer melts[40] where structural transitions of the Landau-Brazovskii type may proceed.[41] For first-order phase transitions, e.g., in solidification phenomena, the average value of ϕ is not zero, and the crystalline state typically invades a metastable phase. In this instance a solvability condition (see, e.g., Ref. 42) is required to determine velocity and wavelength selection. It would be interesting in the future to compare the predictions of this selection criterion for phase field crystal models with the present calculations.

VII. CONCLUSIONS

The present work is devoted to a marginal stability analysis of the parabolic and hyperbolic phase field crystal model in one spatial dimension. Predictions for the front velocity V and selected wave number k_f were presented as a function of undercooling ϵ and relaxation rate τ. It was found that in both parabolic and hyperbolic cases, k_f can differ significantly from the equilibrium value and this difference increases with both undercooling and relaxation rate.

The central result of this work is that for large τ it is possible for the front to select a wave number that is unstable in the bulk phase. This should lead to phase slips occurring at the front or in the bulk depending on how far k_f is above the Eckhaus boundary. The analysis shows that if k_f is just above the Eckhaus boundary then the instability of the perfect periodic state occurs for very long wavelengths at very slow rates. In contrast, when k_f is well above the Eckhaus boundary, then the instability occurs at shorter wavelengths and at a faster rate. It is interesting to speculate on the consequences of this instability for the periodic pattern described by the conserved order parameter (crystal structure) in higher dimensions. In higher dimensions the phase slips correspond to the nucleation of dislocations, thus it is possible that this instability could lead to solids containing many defects or perhaps glassy states. Of course in higher dimensions other interesting phenomena are possible since the front may prefer to select not only a different lattice constant, but could also select a different crystal symmetry than preferred by the bulk phase. These speculations provide motivation for extending this study to higher dimensions. Finally it would also be interesting to apply the analysis to rapid phase transformations in solids both far above and below the transition point.

ACKNOWLEDGMENTS

P.K.G. acknowledges financial support from the German Research Foundation (DFG) under Project No. HE 1601/19 and DLR Space Agency under Contract No. 50WM1140. K.R.E. acknowledges financial support from NSF under Grant No. DMR-0906676.

*Peter.Galenko@dlr.de

[1] W. W. Mullins and R. F. Sekerka, J. Appl. Phys. **35**, 444 (1964).
[2] R. J. Asaro and W. A. Tiller, Metall. Trans. **3**, 1789 (1972); M. Grinfeld, J. Nonlinear Sci. **3**, 35 (1993); Dokl. Akad. Nauk SSSR **290**, 1358 (1986) [Sov. Phys. Dokl. **31**, 831 (1986)].
[3] *Oscillations and Traveling Waves in Chemical Systems*, edited by R. J. Field and M. Burger (Wiley, New York, 1985); D. A. Kessier, J. Koplik, and H. Levine, Adv. Phys. **37**, 255 (1988); P. Pelce, *Dynamics of Curved Fronts* (Academic, Boston, 1988); *Instabilities in Non-equilibrium Structures*, edited by E. Tirapegui and W. Zeller (Kluwer, Dordrecht, 1996); W. van Saarlos, Phys. Rep. **386**, 29 (2003).
[4] M. C. Cross and P. C. Hohenberg, Rev. Mod. Phys. **65**, 851 (1993).
[5] G. Dee and J. S. Langer, Phys. Rev. Lett. **50**, 383 (1983).
[6] K. R. Elder, M. Katakowski, M. Haataja, and M. Grant, Phys. Rev. Lett. **88**, 245701 (2002); K. R. Elder and M. Grant, Phys. Rev. E **70**, 051605 (2004).
[7] J. Swift and P. C. Hohenberg, Phys. Rev. A **15**, 319 (1977); M. C. Cross and P. C. Hohenberg, Rev. Mod. Phys. **65**, 851 (1993).
[8] K. R. Elder, N. Provatas, J. Berry, P. Stefanovic, and M. Grant, Phys. Rev. B **75**, 064107 (2007).
[9] T. V. Ramakrishnan and M. Yussouff, Phys. Rev. B **19**, 2775 (1979); R. Evans, Adv. Phys. **28**, 143 (1979); Y. Singh, Phys. Rep. **207**, 351 (1991).
[10] Y. M. Jin and A. G. Khachaturyan, J. Appl. Phys. **100**, 013519 (2006).
[11] G. Tegze, L. Granasy, G. I. Toth, F. Podmaniczky, A. Jaatinen, T. Ala-Nissila, and T. Pusztai, Phys. Rev. Lett. **103**, 035702 (2009).
[12] G. I. Toth, G. Tegze, T. Pustai, G. Toth, and L. Granasy, J. Phys.: Condens. Matter **22**, 36401 (2010).
[13] S. van Teeffelen, R. Backofen, A. Voigt, and H. Löwen, Phys. Rev. E **79**, 051404 (2009).
[14] J. Berry, M. Grant, and K. R. Elder, Phys. Rev. E **73**, 031609 (2006).
[15] P. Y. Chan, G. Tsekenis, J. Dantzig, K. A. Dahmen, and N. Goldenfeld, Phys. Rev. Lett. **105**, 015502 (2010).
[16] J. Berry, K. R. Elder, and M. Grant, Phys. Rev. E **77**, 061506 (2008).
[17] Z.-F. Huang and K. R. Elder, Phys. Rev. Lett. **101**, 158701 (2008); K.-A. Wu and P. W. Voorhees, Phys. Rev. B **80**, 125408 (2009); Z.-F. Huang and K. R. Elder, *ibid.* **81**, 165421 (2010).
[18] J. Berry, K. R. Elder, and M. Grant, Phys. Rev. B **77**, 224114 (2008); J. Mellenthin, A. Karma, and M. Plapp, *ibid.* **78**, 184110 (2008).

[19]C. V. Achim, M. Karttunen, K. R. Elder, E. Granato, T. Ala-Nissila, and S. C. Ying, Phys. Rev. E **74**, 021104 (2006); C. V. Achim, J. A. P. Ramos, M. Karttunen, K. R. Elder, E. Granato, T. Ala-Nissila, and S. C. Ying, *ibid.* **79**, 011606 (2009); J. A. P. Ramos, E. Granato, S. C. Ying, C. V. Achim, K. R. Elder, and T. Ala-Nissila, *ibid.* **81**, 011121 (2010).

[20]A. Jaatinen, C. V. Achim, K. R. Elder, and T. Ala-Nissila, Phys. Rev. E **80**, 031602 (2009); Tech. Mech. **30**, 169 (2010).

[21]E. Ben-Jacob, H. Brand, G. Dee, L. Kramer, and J. S. Langer, Physica D **14**, 348 (1985).

[22]G. T. Dee and W. van Saarloos, Phys. Rev. Lett. **60**, 2641 (1988); W. van Saarloos, Phys. Rev. A **37**, 211 (1988).

[23]K. R. Elder and M. Grant, J. Phys. A **23**, L803 (1990).

[24]P. Galenko, D. Danilov, and V. Lebedev, Phys. Rev. E **79**, 051110 (2009).

[25]P. Stefanovic, M. Haataja, and N. Provatas, Phys. Rev. Lett. **96**, 225504 (2006); Phys. Rev. E **80**, 046107 (2009).

[26]D. Herlach, P. Galenko, and D. Holland-Moritz, *Metastable Solids from Undercooled Melts* (Elsevier, Amsterdam, 2007).

[27]P. Galenko, Phys. Rev. E **76**, 031606 (2007).

[28]M. Asta (private communication); M. Asta, H. Harith, Y. Yang, S. Deyan, and J. Hoyt, in *Solid-Solid Phase Transformations in Inorganic Materials*, book of abstracts of Conference PTM-2010; June 6-11, 2010, Avignon, France, p. 29.

[29]N. G. De Bruijn, *Asymptotic Methods in Analysis* (North-Holland, Amsterdam, 1961); C. M. Bender and S. A. Orszag, *Advanced Mathematical Methods for Scientists and Engineers* (McGraw-Hill, New York, 1978).

[30]Y. Pomeau and P. Manneville, J. Phys. (Paris), Lett. **40**, L609 (1979).

[31]An approximate analytic solution of Eqs. (13)–(16) is possible for small values of ϵ as shown in Refs. 5 and 21.

[32]P. Galenko and D. Jou, Phys. Rev. E **71**, 046125 (2005).

[33]P. Galenko and D. Jou, Physica A **388**, 3113 (2009).

[34]N. Lecoq, H. Zapolsky, and P. Galenko, Eur. Phys. J. Special Topics **177**, 165 (2009); P. Galenko, D. Kharchenko, and I. Lysenko, Physica A **389**, 3443 (2010).

[35]D. Jou, J. Casas-Vazquez, and G. Lebon, *Extended Irreversible Thermodynamics*, 4th Ed. (Springer, Berlin, 2010).

[36]Indeed, rewriting Eq. (30) in the alternative form of $\tau\omega^2 + \omega = \alpha(k) + ikV(1 + 2\tau\omega)$, one can explicitly see that the term $2\tau\omega$ is not negligible in comparison with unity at large values of ω.

[37]K. Elder, *Lecture Notes on Phase Field Modeling*, preprint of DFG-German Research Foundation Summer School on Priority Programme SPP-1296 (DFG, Aachen, 2008).

[38]The equilibrium value of k is always very close to 1. Near $\epsilon = 0$ Pomeau and Manneville (Ref. 30) have shown $k \approx 1 - \epsilon^2/1024$.

[39]W. Eckhaus, *Studies in Nonlinear Stability Theory* (Springer, Berlin, 1965); L. S. Tuckerman and D. Barkley, Physica D **46**, 57 (1990).

[40]L. Leibler, Macromolecules **13**, 1602 (1980); T. Ohta and K. Kawasaki, *ibid.* **19**, 2621 (1986).

[41]S. K. Mkhonta, K. R. Elder, and M. Grant, Eur. Phys. J. E **032**, 349 (2010).

[42]B. Echebarria, R. Folch, A. Karma, and M. Plapp, Phys. Rev. E **70**, 061604 (2004).